

Probabilistic Small Signal Stability Analysis of Autonomous Wind-Diesel Microgrid

Awan Uji Krismanto

School of Information Technology and Electrical
Engineering
University of Queensland, Australia

N. Mithulanathan

School of Information Technology and Electrical
Engineering
University of Queensland, Australia

Abstract—Probabilistic analysis of small signal stability analysis of a Hybrid Microgrid (MG) consists of two Wind Energy Conversion System (WECS) and one Diesel Engine (DE) is presented. As wind speed varied, active power output from WECS based distributed generator (DG) changed proportionally. The fluctuation of power contribution from each DG units significantly affects the oscillatory stability in MG. Therefore, to manage the uncertain condition of wind speed, a conventional droop control method should be modified. In this paper, the modified droop control method is employed to observe the small signal stability performance of hybrid MG under wind speed uncertainty. Probabilistic small signal stability of the MG system when the WECS based DG units were subjected to the same and different wind speed regimes were investigated using Monte Carlo (MC) method. Statistical analysis of the critical eigenvalues trajectories, damping ratio and oscillatory frequency are thoroughly analysed and presented. It was observed that at a higher wind speed variation, the small signal stability performance of MG deteriorated severely. Moreover, it was also monitored that when each of WECS was subjected to distinct wind speed, the system stability declines considerably, compared to when same wind speed regime was applied on each of those WECS based DG units.

Keywords—Microgrid, uncertainty, probabilistic, small signal stability.

I. INTRODUCTION

Penetration of renewable energy resources (RES) based DG in a microgrid (MG) system has increased remarkably, specifically to provide environmentally friendly and reliable electricity service for remote areas. Among various RES, wind energy has received significant attention due to its technical and economic benefits. Since the characteristics of WECS is different from the conventional synchronous generator, it introduces novel challenges in system operation. The generated power from WECS varies accordingly, depending on wind speed. As a result, the balanced condition of power generation and load demand might be disturbed. The change in power balance could significantly affect the system stability, leaning to weaken the critical modes. Trajectories of sensitive eigenvalues would change considerably, deteriorating the system dynamic response.

Conventionally, investigation of the oscillatory condition and small signal stability is conducted through modal analysis based on deterministic approach. However, the deterministic

method is unable to capture the stochastic features corresponding to the RES uncertainties [1]. To overcome this limitation, the probabilistic approach in monitoring oscillatory stability in the power system is considered. Many studies have been extensively conducted to investigate the small signal stability of large power system with high penetration of WECS. In [1-4], the probabilistic distribution of critical modes related to local and inter-area eigenvalues was monitored. It was found that increasing penetration of wind power significantly influenced the system stability. Moreover, a variation of generated power from wind farm affected the power transfer in the interconnected power system. In [5, 6], The small signal stability index was introduced to assess the probabilistic stability performance in different power transfer and wind generation level. However, only few work has been reported to investigate the probabilistic small signal stability in autonomous MG operation due to uncertain condition of RES.

In this paper, the small signal stability performance of autonomous hybrid MG comprising of WECS and diesel engine (DE) is investigated. A comprehensive model of the wind and DE-based DGs with their associated controller are developed. The probability of small signal stability performance corresponded to the distribution of critical eigenvalues and damping ratio would be observed based on the estimated random wind speed variation. MC simulation is performed to generate a certain number of random samples from the estimated probability density function (*pdf*) of actual wind speed.

The remainder of the paper is organised as follows. Estimation procedure of *pdf* of the wind speed from the available data is presented in Section II. In Section III, a complete system modelling of DE and WECS DG units involving dynamic models of the control system, distribution network and load are presented. The simulation results are presented and discussed in Section IV. Eventually, conclusions and contributions of this paper are highlighted in Section V.

II. WIND SPEED MODEL AND MONTE CARLO SIMULATION

A. Wind Speed Model

In this paper, simulated wind speed regime is derived from annual wind speed data in 30 minutes resolution. The probabilistic $f(v)$ and cumulative $F(v)$ distribution functions of

wind speed can be presented using Weibull distribution function as given by (1) and (2).

$$f(v) = \frac{k}{c} \left(\frac{v}{c}\right)^{k-1} \exp\left[-\left(\frac{v}{c}\right)^k\right] \quad (1)$$

$$F(v) = 1 - \exp\left[-\left(\frac{v}{c}\right)^k\right] \quad (2)$$

Where v represents wind speed in m/s; k and c are related to shape and scale parameters of the Weibull function.

The parameters of Weibull function can be determined through numerical methods such as *maximum likelihood method* [7]. In this approach, the Weibull parameters can be calculated according to (3) and (4).

$$k = \left[\frac{\sum_{i=1}^n v_i^k \ln(v_i)}{\sum_{i=1}^n v_i^k} - \frac{\sum_{i=1}^n \ln(v_i)}{n} \right]^{-1} \quad (3)$$

$$c = \left(\frac{1}{n} \sum_{i=1}^n v_i^k \right)^{\frac{1}{k}} \quad (4)$$

Where n is the number of observations performed.

After estimating the parameters of Weibull *pdf*, wind speed samples are then generated according to its probabilistic distribution. The power output of WECS based DGs can be determined by applying the wind speed data series to the following equation

$$P_{opt} = 0.5 \rho C_{opt} (\lambda_{opt}, \beta) A_r v_w^3 \quad (5)$$

With ρ is the air density (kg/m^3), v_w is wind speed (m/s), A_r is the effective area covered by turbine blades in (m^2) and C_{opt} is the optimal power coefficient of a wind turbine for a certain wind speed. While λ_{opt} and β respectively represent tip speed ratio and blade pitch angle in degree.

B. Monte Carlo (MC) Simulation for Small Signal Stability

MC method is a repetitive procedure that evaluates the system response iteratively using a set of input variables which are generated randomly from their probabilistic distribution function (*pdf*). Probabilistic study of small signal stability in MG may be conducted by evaluating all the possible operating conditions due to the variation of wind speed. The procedure of probabilistic small signal stability using MC method is depicted in Fig.1 [4, 8].

The MC simulation is started by developing a complete dynamic small signal model of the hybrid MG considering wind speed variation. A random sample of wind speed will be generated according to the estimated *pdf* wind speed model. From the sampled wind speed data, the operating point is determined. Calculation of system eigenvalues based on modal analysis method is conducted next. Finally, the statistical analysis corresponding to the probabilistic behaviour of critical eigenvalues and system stability performance can be carried out.

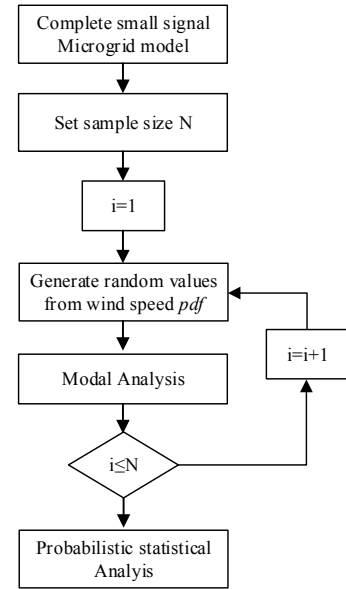


Fig.1 Procedure of small signal stability analysis with MC method.

III. HYBRID MICROGRID MODEL

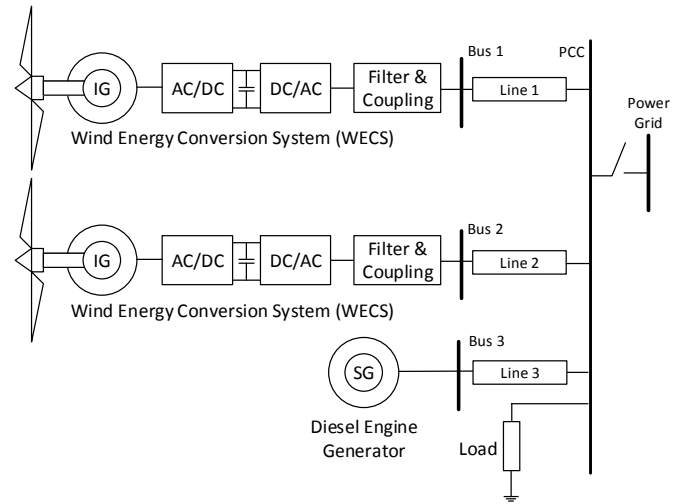


Fig. 2. Hybrid microgrid model.

Fig.2 shows the investigated hybrid MG model that consists of three DG units and a central load. Two fully rated WECS type with back-to-back (AC/DC/AC) inverter were considered in the MG. The Diesel Engine (DE) based DG is then integrated to ensure power balance due to lack of RES power from WECS. Moreover, the DE provides a reference value for the synchronisation process among DGs. State space model of the line impedance and static load are derived from [9].

A. Diesel Engine (DE) Generator Model

Detailed state space model of DE generator is derived from [10, 11]. State variables of DE, consist of rotor, stator, and field winding currents in the d - q axis. While, input variables are presented as mechanical torque, field winding, and stator voltage. State space equation of DE generator is stated as given in (6).

$$\dot{\Delta x}_{de} = A_{de} \Delta x_{de} + B_{de} \Delta u_{de} + B_{vde} \Delta v_{b3} \quad (6)$$

Where

$$\Delta x_{de} = [\Delta i_{sd}, \Delta i_{sq}, \Delta i_{fd}, \Delta i_{kd}, \Delta i_{kq1}, \Delta i_{kq2}, \Delta \omega_{ref}, \Delta \delta_{ref}]^T$$

$$\Delta u_{de} = [\Delta v_{fd}, \Delta T_{Mde}]^T, \Delta v_{b3} = [\Delta v_{b3dq}]^T$$

B_{de} and B_{vde} represent input and connection matrices between DE-local bus, respectively.

B. WECS Model

Small signal model of wind turbine, induction generator in WECS are derived from [10, 12]. While AC/DC/AC converter model is obtained from [13-15]. The control scheme in WECS is comprising of generator and grid side converter control. The flux oriented control (FOC) strategy in generator side converter is responsible for regulation of DC link voltage [12]. Detailed control model of generator side converter is adapted from [16]. The grid side inverter consists of primary and secondary controllers is depicted in Fig. 3 [9, 17]. The primary control which employed modified droop control method is responsible for providing a power-sharing scheme, frequency and voltage regulation. While, the secondary control comprising of voltage and current control loop is in charge of compensating voltage and frequency deviations, improving dynamic response and providing a control signal for the inverter.

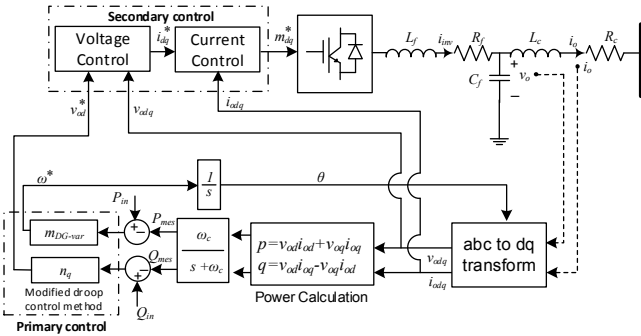


Fig. 3. Power Circuit and proposed modified droop control of DG units grid side inverter within microgrid.

Static droop control provides frequency and voltage reference values as dictated in (7) and (8).

$$\omega = \omega^* - m_p \Delta P_{meas} \quad (7)$$

$$v = v^* - n_q \Delta Q_{meas} \quad (8)$$

Where ω^* and v^* are the set point reference for frequency and voltage.

Measured average active (ΔP_{meas}) and reactive (ΔQ_{meas}) power are determined by implementing one order low pass filter as given in (9).

$$\Delta P_{meas} = \frac{\omega_c}{s + \omega_c} p \rightarrow \frac{d\Delta P_{meas}}{dt} = \omega_c p - \omega_c \Delta P_{meas} \quad (9)$$

$$\Delta Q_{meas} = \frac{\omega_c}{s + \omega_c} q \rightarrow \frac{d\Delta Q_{meas}}{dt} = \omega_c q - \omega_c \Delta Q_{meas} \quad (10)$$

A modified droop control which can dynamically adjust the power-sharing scheme among DG units is proposed to handle the variation of wind speed. With the modified droop, the power distribution scheme adaptively changes by wind speed changes. It is assumed that power input from a particular wind speed condition is a function of a given wind speed with constant tip speed ratio and blade pitch angle. By considering the generated wind power from (5), the modified active droop gain control of a WECS is given (11).

$$m_{WECS-var} = m_{max} - (m_{max} - m_{min}) \left\{ \frac{0.5 \rho C_{opt} (\lambda_{opt}, \beta) A_r v_{w0}^3}{P_{max}} \right\} \quad (11)$$

Where v_{w0} represents an initial condition of wind speed around a certain operating point.

Active and reactive droop gains selections are evaluated as a compromise among accurate power-sharing, enhancement of dynamic response and voltage regulation. However, since the MG stability less sensitive to reactive droop gain variation, the reactive power droop gain of each DG unit is maintained at constant value [18].

The obtained reference values from primary control become input variables for secondary control. It consists of outer voltage and inner current controller loop. Voltage controller is responsible for generating reference values for inner current loop and synthesise reference filter-inductor current vector [19]. Eventually, modulation and switching signal for VSI (m_{dq}^*) is determined from the current controller loop.

State space equation of the droop and voltage controller are adopted from [9]. While the corresponding state equations of voltage and current controller are given by (12) and (13) respectively.

$$\begin{aligned} \begin{bmatrix} \Delta \dot{\phi}_{dq} \\ \dot{v}_{dq} \end{bmatrix} &= \begin{bmatrix} 0 \\ 0 \end{bmatrix} \begin{bmatrix} \Delta \phi_{dq} \\ v_{dq} \end{bmatrix} + \begin{bmatrix} 1 & 0 & -1 & 0 \\ 0 & 1 & 0 & -1 \end{bmatrix} \begin{bmatrix} v_{odq}^* \\ v_{odq} \end{bmatrix} \\ \begin{bmatrix} \dot{i}_{dq}^* \\ \dot{v}_{odq} \end{bmatrix} &= \begin{bmatrix} K_{iv} & 0 \\ 0 & K_{iv} \end{bmatrix} \begin{bmatrix} \Delta \phi_{dq} \\ v_{dq} \end{bmatrix} + \begin{bmatrix} K_{pv} & 0 & -K_{pv} & -\omega C_f \\ 0 & K_{pv} & \omega C_f & -K_{pv} \end{bmatrix} \begin{bmatrix} v_{odq}^* \\ v_{odq} \end{bmatrix} \end{aligned} \quad (12)$$

$$\begin{aligned} \begin{bmatrix} \Delta \dot{\beta}_{dq} \\ \dot{i}_{odq}^* \\ \dot{i}_{odq} \end{bmatrix} &= \begin{bmatrix} 0 \\ 0 \\ 0 \end{bmatrix} \begin{bmatrix} \Delta \beta_{dq} \\ i_{odq}^* \\ i_{odq} \end{bmatrix} + \begin{bmatrix} 1 & 0 & -1 & 0 \\ 0 & 1 & 0 & -1 \end{bmatrix} \begin{bmatrix} i_{odq}^* \\ i_{odq} \end{bmatrix} \\ \begin{bmatrix} \dot{m}_{dq}^* \\ \dot{i}_{odq} \end{bmatrix} &= \begin{bmatrix} K_{ic} & 0 \\ 0 & K_{ic} \end{bmatrix} \begin{bmatrix} \Delta \phi_{dq} \\ v_{dq} \end{bmatrix} + \begin{bmatrix} K_{pc} & 0 & -K_{pc} & -\omega L_f \\ 0 & K_{pc} & \omega L_f & -K_{pc} \end{bmatrix} \begin{bmatrix} i_{odq}^* \\ i_{odq} \end{bmatrix} \end{aligned} \quad (13)$$

Where ϕ_{dq} and β_{dq} respectively represent auxiliary state variables of voltage and controller loop.

A complete model for fully rated converter WECS is then derived by integrating state equations of induction generator [10, 20], back to back inverter [14, 15], FOC at generator side and droop controller at grid side converter [9, 16]. Moreover, detailed modelling procedure of both controllers can be obtained in [9, 12, 17, 20, 21]. State space equation of WECS is given in (14).

$$\dot{\Delta x}_w = A_w \Delta x_w + B_w \Delta u_w + B_{vw} \Delta v_{b1} + B_{wd} \Delta \omega_{ref} \quad (14)$$

$$\Delta x_w = \begin{bmatrix} \Delta i_{sdq} & \Delta i_{rdq} & \Delta \omega_{rw} & \Delta \gamma & \Delta \rho_{wdq} & \Delta i_{dq} & \Delta v_{indq} \\ \Delta \delta_w & \Delta P_w & \Delta Q_w & \Delta \varphi_{dq} & \Delta \beta_{dq} & \Delta v_{dcout} & \Delta i_s \\ \Delta v_{dc} & \Delta i_{invdq} & \Delta v_{odq} & \Delta i_{odq} \end{bmatrix}^T$$

Where

In which, γ and ρ_{wdq} are the auxiliary variables for FOC controller. B_w is input matrix of WECS. Connection matrices of WECS to the line and DE are given by B_{vw} and B_{wd} respectively.

IV. RESULTS AND DISCUSSIONS

A. Wind Speed Estimation

The 30 minutes resolution of annual wind speed data from four different regions in Australia was considered. Fig.4 illustrates the probabilistic distribution of wind speed in four wind regimes. The histogram charts indicate the probabilistic occurrence of a particular wind speed in a specified region.

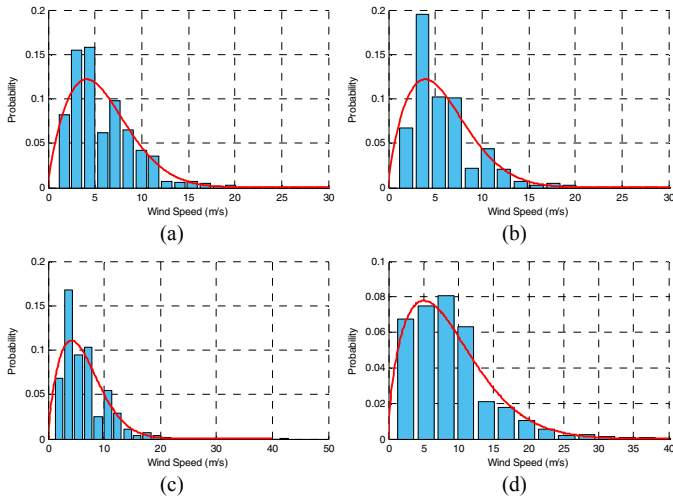


Fig. 4. Pdf of the actual wind speed from regime (a) 1, (b) 2, (c) 3 and (d) 4.

From the collected data, the parameters of Weibull distribution function were determined using *maximum likelihood method*. Calculation of these parameters was conducted using Statistical Toolbox in MATLAB. The obtained parameters were then utilised for estimating the *pdf* of the wind speed. From the estimated *pdf*, 1000 samples of random wind speed values were generated. Finally, the generated wind velocity data were randomly sampled through MC simulation to realise the practical scenario of wind uncertainties. The estimated wind speed data set for the MC simulation is presented in Fig.5.

Statistical analysis corresponding to the average and standard deviation of the actual and estimated wind velocity is shown in Table 1. Less than 5% difference of mean and standard deviation values between actual and estimated wind speed data was observed. Hence it can be considered that Weibull distribution function was able to estimate the *pdf* of wind velocity. Moreover, It was clearly shown that the least and the most fluctuated wind speed condition were monitored in regions 1 and 4 respectively, indicated by the lowest and the

highest standard deviation from the actual and estimated wind velocity data.

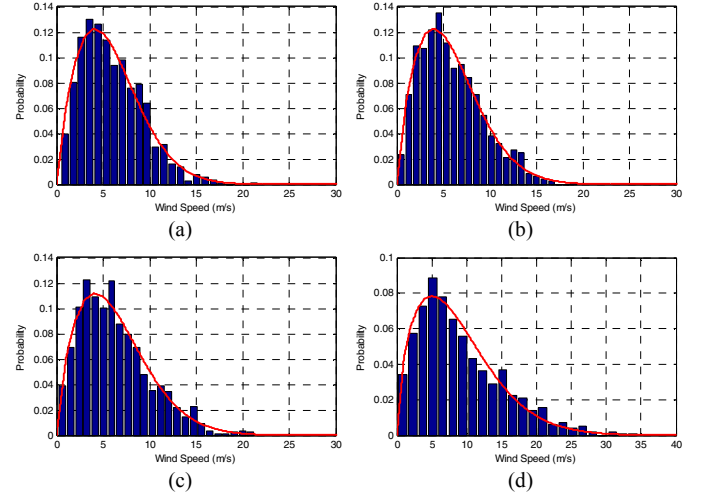


Fig. 5. Pdf of the estimated wind speed from the regime (a) 1, (b) 2, (c) 3 and (d) 4.

Table 1. Statistical analysis in four wind speed regimes.

Wind Regime	Mean		Err. (%)	St. Deviation		Err. (%)
	Act.	Est.		Act.	Est.	
1	6.081	5.879	3.31	3.553	3.392	4.52
2	6.016	5.821	3.23	3.609	3.457	4.21
3	6.512	6.334	2.75	3.987	3.801	4.69
4	9.002	8.709	2.57	6.054	5.789	4.37

In this paper, two main study cases of wind speed uncertainties are considered. The first study case assumed that WECS1 and WECS2 were subjected to similar wind speed. Hence there are four different scenarios (one each for each wind regime) for this study case. In the second study case, it was considered that WECS1 and WECS2 experienced different wind speed situations. Three wind speed combinations from regions 1&4, 2 & 4 and 3&4 were applied to WECS1 and WECS2 respectively.

B. Probabilistic Small Signal Stability

A complete state space model of two WECS and one DE-based DG units in a hybrid MG architecture was constructed. Two WECS and one DE-based DGs with each capacity of 3 MVA were integrated to supply a 5 MW load through lines impedance model of the distribution network. Parameters of induction machine and permanent magnet generator for WECS and DE were derived from [10, 16, 20]. The full 72 order state matrix was developed to realise the small signal model of the MG incorporating state equations of each of the DG units and its associated controllers, line impedance and constant load.

Assessment of oscillatory condition in various power-sharing schemes is crucial to determine stability boundary of MG operation. The generated power from WECS is highly correlated to the uncertain state of wind speed. Hence, power-sharing scheme among DG units was significantly influenced by wind speed change. To incorporate wind uncertainty in modal analysis, wind speed variation was reflected in input power and droop gain controller state equations. To deal with

wind speed variation, a modified droop control strategy was proposed. The active power droop gain was adjusted according to the change of wind speed by using equation (11). In this paper, a maximum and minimum active power droop were set at 8% and 4%, respectively. Dynamic behaviour of the critical modes associated with power output from WECS is thoroughly investigated. Eigen-trajectories and statistical analysis of the critical modes are presented to evaluate the small signal stability performance of MG.

First study case has considered similar wind speed data series for WECS1 and WECS2. Fig.6 shows the trajectories of sensitive modes corresponding to the active power output of WECS when same wind speed regime from different regions was implemented to both WECS. According to a statistical characteristic of the pre-set wind speed data in Table 1, higher standard deviation indicated the more fluctuating condition of wind speed. The eigen-trajectories results show that small variation of the critical modes was monitored when both the WECS units were subjected to the less fluctuated wind speed in region 1. As the wind velocities in regime 2 to 4 was more fluctuated than regime 1, the system small signal stability deteriorated significantly. The investigated modes departed significantly to the right-hand side of the complex plane, indicate a more oscillatory condition and an increase of possible instability events.

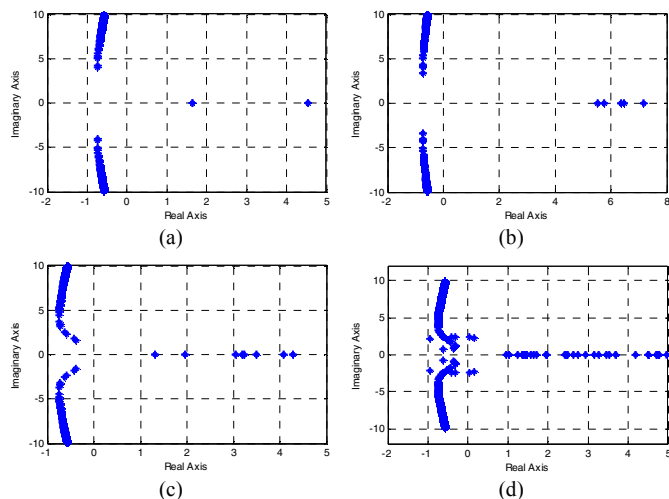


Fig. 6. Eigenvalues trajectories when similar wind speed of regime (a) 1, (b) 2, (c) 3 and (d) 4 are applied to both WECS 1 and WECS 2.

Table 2. Statistical analysis of critical modes in four wind speed regimes.

Wind regime		Damping ratio		Frequency of oscillation		Stable Prob.(%)
WECS1	WECS2	Mean	Std.	Mean	Std.	
1	1	0.0608	0.057	9.455	0.891	99.7
2	2	0.0578	0.081	9.431	1.091	99.4
3	3	0.0566	0.097	9.233	1.369	99.1
4	4	0.0285	0.356	7.903	3.112	92.7

Statistical analysis of the investigated modes in similar wind speed scenarios is presented in Table 2. From this table, it was observed that when WECS1 and WECS2 were subjected to similar wind velocity regimes, the stable condition of MG can be maintained. Only few instability

events occurred. The instability emerged when WECS were subjected to wind speed higher than 15 m/s. It was monitored that when both of WECSs were subjected to 4th wind speed regime, higher deviation of damping ratio and oscillatory frequency of critical modes were monitored, denoting the more fluctuated condition of the critical modes.

In second study case, it was considered that WECS1 and WECS 2 were subjected to different wind velocity. Three wind speed combinations from regimes 1&4, 2&4 and 3&4 were applied to WECS1 and WECS2 respectively. Fig.7 depicts the dynamic behaviour of the critical modes in three wind speed combinations.

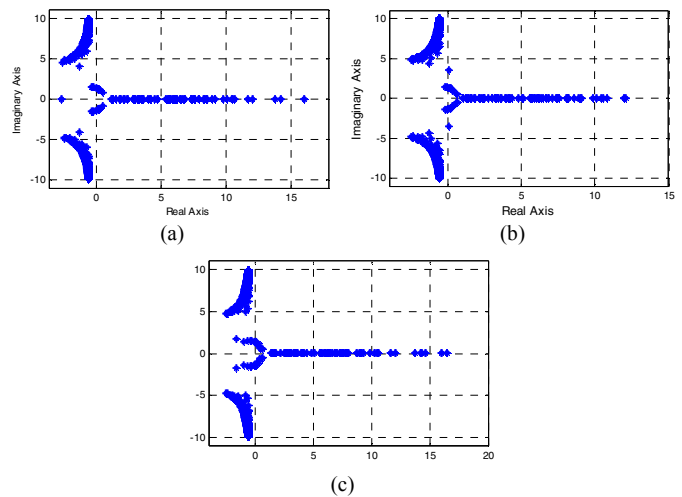


Fig. 7. Eigenvalues trajectories when a combination of wind speed of regime (a) 1-4, (b) 2-4, (c) 3-4 are applied to WECS 1 and WECS 2 respectively.

In the first study case, generated power from each of WECS was similar, since it was assumed that same wind speed was experienced by every WECS. Hence, the contribution of each RES based DG unit to power-sharing was equal, and droop gain setting of each WECS would be identical. As a result, less fluctuated dynamic behaviour of the critical modes was observed. However, when different wind speed is experienced, the droop control in each WECS responded differently. Hence the power contribution from each WECS would be different. More oscillatory conditions were experienced, indicated by more dispersed trajectories of eigenvalues. Significant right eigenvalues movements were monitored, resulting in the deterioration of system damping and stability margin. The risk of unstable situation occurred frequently, indicated by more eigenvalues trajectories located on the right half complex plane.

The frequency distribution of calculated damping ratio based on estimated wind speed data series is given in Fig. 8. More than 800 (80%) events with the damping ratio around 0.077 (7.7%) were monitored in three different wind speed combinations. The statistical analysis of stability indicated that the hybrid MG could handle most of the wind speed fluctuations. However, it was also observed that around 87 (8.6%) instability events took place. The unstable situation increased slightly to 9.2% when a combination of wind speed from regime 3 and 4 was considered.

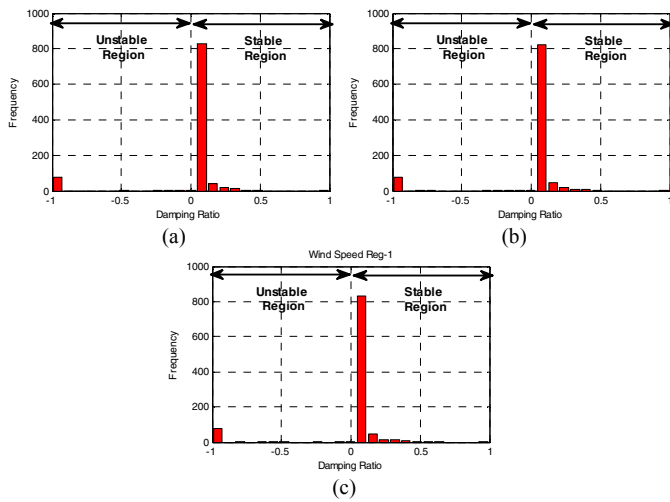


Fig. 8. Distribution of damping ratio when a combination of wind speed of (a) 1-4, (b) 2-4, (c) 3-4 are applied to WECS 1 and WECS 2 respectively.

Statistical analysis of the critical eigenvalues in three different combinations of wind speed is presented in Table 3. The probability of stable operation can be maintained around 91%. While the occurrence of unstable events was kept below 10%. It also notable that compared to the previous identical wind speed scenario, the stability performance decreased slightly from around 99% to 91%. The exemption was made in the fourth case of similar wind speed regimes scenario. In this case, the stability was relatively similar to the combination scenarios. It could happen since, in 4&4 wind speed case, the average wind speed was higher than the other case. Hence more fluctuating condition would be experienced.

Table 3. Statistical features of critical modes in three wind combinations.

Wind regime		Damping ratio		Frequency of oscillation		Stable Prob.(%)
WECS1	WECS2	Mean	Std.	Mean	Std.	
1	4	0.075	0.12	8.25	2.79	91.59
2	4	0.078	0.08	8.21	2.77	91.19
3	4	0.077	0.11	8.15	2.78	90.05

V. CONCLUSIONS

In this paper, a probabilistic small signal stability analysis of hybrid wind-diesel MG was presented. To manage with the wind speed change, modified droop control method was proposed. Eigen-trajectories and statistical analysis suggested that at higher wind speed, the small signal stability performance of MG declined severely. Moreover, it was also monitored that the oscillatory stability deteriorated considerably when each of WECS based DG units in MG were subjected to different wind speed compared to when similar wind speed regime was applied in each DG units.

REFERENCES

[1] H. Ahmadi and H. Seifi, "Probabilistic tuning of Power System Stabilizers considering the wind farm generation uncertainty," *Electrical Power and Energy Systems*, vol. 63, pp. 565-576, 2014.

[2] S. Q. Bu, W. Du, H. F. Wang, Z. Chen, L. Y. Xiao, and H. F. Li, "Probabilistic Analysis of Small-Signal Stability of Large-Scale Power Systems as Affected by Penetration of Wind Generation," *IEEE Transaction on Power System*, vol. 30, pp. 2479-2486, 2012.

[3] H. Yue, G. Li, and M. Zhou, "A Probabilistic Approach to Small Signal Stability Analysis of Power Systems with Correlated Wind Sources," *Journal Electrical Engineering Technology*, vol. 8, pp. 742-751, 2013.

[4] L.-B. Shi, L. Kang, L.-Z. Yao, S.-Y. Qin, R.-M. Wang, and J.-P. Zhang, "Effects of Wind Generation Uncertainty and Volatility on Power System Small Signal Stability," *Journal Electrical Engineering Technology*, vol. 90, pp. 60-70, 2014.

[5] U. Kerin, T. N. Tuan, E. Lerch, and G. Bizjak, "Small Signal Security Index for Contingency Classification in Dynamic Security Assessment," presented at the IEEE Power Tech., Trondheim, 2011.

[6] J. L. Rueda and D. G. Colomé, "Probabilistic performance indexes for small signal stability enhancement in weak wind-hydro-thermal power systems," *IET Generation, Transmission & Distribution*, 2009.

[7] P. A. C. Rocha, R. C. d. Sousa, Carla Freitas de Andrade, and M. E. V. d. Silva, "Comparison of seven numerical methods for determining Weibull parameters for wind energy generation in the northeast region of Brazil," *Applied Energy*, vol. 89, pp. 395-400, 2012.

[8] J. L. Rueda, D. G. Colomé, and I. Erlich, "Assessment and Enhancement of Small Signal Stability Considering Uncertainties," *IEEE Transaction on Power System*, vol. 24, 2009.

[9] N. Pogaku, M. Prodanovic, and T. C. Green, "Modeling, analysis and testing of autonomous operation of an inverter-based microgrid," *IEEE Transactions on Power Electronics*, vol. 22, pp. 613-625, Mar 2007.

[10] P. C. Krause, O. Wasynczuk, and S. D. Sudhoff, *Analysis of Electric Machinery and Drive System 2nd Edition*: Wiley-Interscience, 2002.

[11] C. E. Ugalde-Loo and J. B. Ekanayake, "State-Space Modelling of Variable-Speed Wind Turbines: A Systematic Approach," presented at the Sustainable Energy Technologies (ICSET), Kandy, Sri Lanka, 2010.

[12] O. Anaya-Lara, N. Jenkins, J. Ekanayake, P. Cartwright, and M. Hughes, *Wind Generation: Modelling and Control*: John Wiley & Sons, Ltd, 2009.

[13] R. Wu, S. B. Dewan, and G. R. Slemmon, "A Pwm Ac-to-Dc Converter with Fixed Switching Frequency," *Ieee Transactions on Industry Applications*, vol. 26, pp. 880-885, Sep-Oct 1990.

[14] R. Wu, S. B. Dewan, and G. R. Slemmon, "Analysis of an AC-to-DC Voltage Source Converter using PWM with Phase and Amplitude Control," *IEEE Transactions on Industry Application*, vol. 27, p. 12, 1991.

[15] N. A. Rahim and J. E. Quaicoe, "Small Signal Model and Analysis of A Multiple Feedback Control Scheme for Three Phase Voltage Source UPS Inverter," in *Proceedings of Power Electronics Specialist Conference*, Bovenno, Italy, 1996, pp. 188-194.

[16] BinWu, Y. Lang, N. Zargari, and S. Kouro, *Power Conversion and Control of Wind Energy Systems*: Wiley, 2011.

[17] A. Kahrobaei and Yasser Abdel-Rady I. Mohamed, "Analysis and Mitigation of Low-Frequency Instabilities in Autonomous Medium-Voltage Converter-Based Microgrids With Dynamic Loads," *IEEE Transaction on Industrial Electronics*, vol. 61, pp. 1643-1658, 2014.

[18] E. Barklund, N. Pogaku, M. Prodanovic, C. Hernandez-Aramburo, and T. C. Green, "Energy Management in Autonomous Microgrid Using Stability-Constrained Droop Control of Inverters," *IEEE Transaction on Power Electronics*, vol. 23, pp. 2346-2351, 2008.

[19] Y. A.-R. I. Mohamed and E. F. El-Saadany, "Adaptive Decentralized Droop Controller to Preserve Power Sharing Stability of Paralleled Inverters in Distributed Generation Microgrids," *IEEE Transaction on Power Electronics*, vol. 23, pp. 2806-2816, 2008.

[20] C. E. Ugalde-Loo, J. B. Ekanayake, and N. Jenkins, "State-Space Modeling of Wind Turbine Generators for Power System Studies," *IEEE Transactions on Industry Application*, vol. 48, pp. 223-232, 2013.

[21] A. U. Krismanto and M. Nadarajah, "Identification of Modal Interaction and Small Signal Stability in Autonomous Microgrid Operation," *IET Gen. Transm. Distrib.*, 2017.